

## Potent Inhibitor Design Against H1N1 Swine Influenza: Structure-based and Molecular Dynamics Analysis for M2 Inhibitors from Traditional Chinese Medicine Database

<http://www.jbsdonline.com>

**Chia-Hui Lin<sup>1</sup>**  
**Tung-Ti Chang<sup>2, 8</sup>**  
**Mao-Feng Sun<sup>3, 8</sup>**  
**Hsin-Yi Chen<sup>4</sup>**  
**Fuu-Jen Tsai<sup>4,5</sup>**  
**Kun-Lung Chang<sup>6</sup>**  
**Mark Fisher<sup>7</sup>**  
**Calvin Yu-Chian Chen<sup>4,7,8,9\*</sup>**

<sup>1</sup>Department of Chinese Medicine, China  
Medical University Hospital, Taiwan

<sup>2</sup>Department of Chinese Pediatrics, China  
Medical University Hospital, Taiwan

<sup>3</sup>Department of Acupuncture, China  
Medical University Hospital, Taiwan

<sup>4</sup>Department of Bioinformatics, Asia  
University, Taichung, 41354, Taiwan

<sup>5</sup>Department of Medical Genetics,  
Pediatrics and Medical Research, China  
Medical University Hospital and College  
of Chinese Medicine, China Medical  
University, Taichung, 40402, Taiwan

<sup>6</sup>Department of Pharmacy, China  
Medical University Hospital, Taichung,  
40402, Taiwan

<sup>7</sup>Harvard-MIT Division of Health  
Sciences and Technology, 77  
Massachusetts Avenue, Cambridge,  
MA 02139, USA

\*Phone: +1-617-353-7123  
E-mail: [ycc@mail.cmu.edu.tw](mailto:ycc@mail.cmu.edu.tw); [ycc929@MIT.EDU](mailto:ycc929@MIT.EDU) (C.Y.-C. Chen)

### Abstract

The rapid spread of influenza virus subtype H1N1 poses a great threat to million lives worldwide. To search for new anti-influenza compounds, we performed molecular docking and molecular dynamics simulation to identify potential traditional Chinese medicine (TCM) constituents that could block influenza M2 channel activity. Quinic acid, genipin, syringic acid, cucurbitine, fagarine, and methyl isoferulate all have extremely well docking results as compared to control amantadine. Further *de novo* drug design suggests that derivatives of genipin and methyl isoferulate could have enhanced binding affinity towards M2 channel. Selected molecular dynamics simulations of M2-derivative complexes show stable hydrogen bond interactions between the derivatives and M2 residues, Ser10 and Ala9. To our best knowledge, this is the first study on the anti-viral activity of the above listed TCM compounds.

Key words: H1N1; M2 proton channel; Docking; Molecular dynamics; Traditional Chinese medicine (TCM).

### Introduction

The recent H1N1 influenza pandemic has attracted worldwide attention due to the high infection rate. Oseltamivir (Tamiflu) and zanamivir (Relenza), both of which have been effective in treating influenza A in the past, are recently found to be ineffective against mutated strains (1). Therefore, there is an urgent need to search for new effective anti-viral compounds.

In addition to hemagglutinin and neuraminidase, the surface membrane of influenza virus A still consist a M2 proton channel. M2 is a homotetrameric protein that is constituted by an N-terminal periplasmic domain, a transmembrane (TM) domain, and a C-terminal cytoplasm tail (2). This proton channel is activated by low pH environment in the endosome. The inflow of proton through

<sup>8</sup>Laboratory of Computational and Systems Biology, School of Chinese Medicine, China Medical University, Taichung, 40402, Taiwan

<sup>9</sup>Computational and Systems Biology, Massachusetts Institute of Technology, Cambridge, MA 02139, USA

M2 acidifies the interior environment of the virus, leading to the dissociation of viral matrix protein (M1) from viral RNA genome (2). The activation site of M2 protein is believed to be in the transmembrane domain, with the ionizable His37 acts as the pH sensor and the indole side chain of Try41 acts as a the channel gate (3, 4).

Amantadine and rimantadine are both commercial available adamantane-based drugs used in the past for treating influenza A. However, the effectiveness of these drugs is now greatly debated due to the high number of adamantane inhibitor resistant influenza viral strains (5, 6). Recently, two groups have simultaneously published their high-resolution structures of the M2 transmembrane domain in the presence adamantane inhibitors.

The main focus in this research is to discover potential natural compounds that can directly block the M2 proton channel from allowing entry of hydrogen ions. In recent years, computer-aided drug design (CADD) has been a promising strategy for identifying potential lead compounds and molecular structural features that are related to biological activity. Structure-based investigations have been widely used to study ligand and receptor interaction and have been applied in drug designs (7-16). Molecular dynamics simulation, too, has been widely applied to investigate biological systems (17-31). In the past, our group has been a pioneer in developing new scoring function (32) and also has successfully implemented CADD technology into development of new therapeutics (33-52). Thus, we hope to combine our experiences in structure-based drug design and molecular dynamics simulation to study M2 proton channel. An experiment scheme for this study is shown in Figure 1.

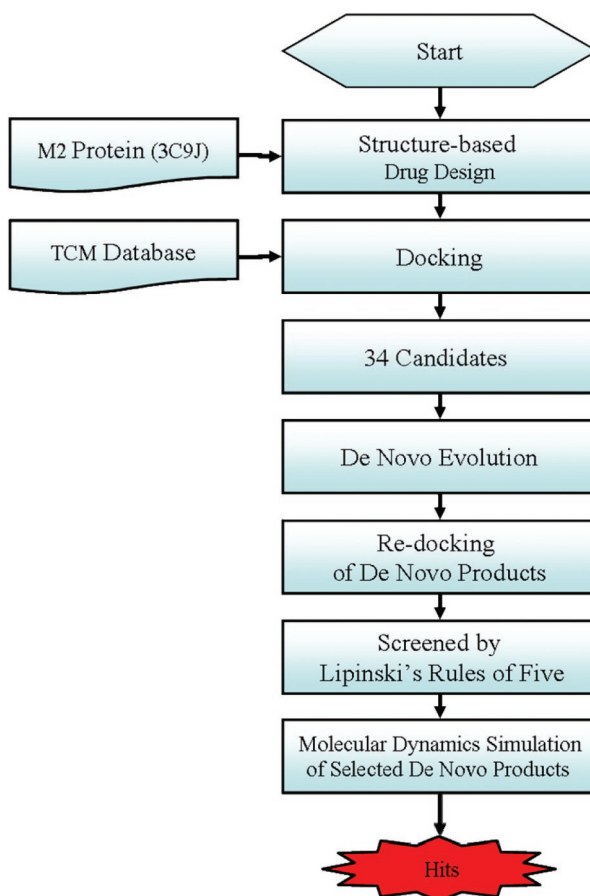


Figure 1: The overall experiment design.

### Dataset

We have created a small molecule database (<http://tcm.cmu.edu.tw/>) containing three-dimensional structures of compounds isolated from traditional Chinese medicine (TCM). These TCM compounds were obtained from extensive literature searches and were drawn into two-dimensional and three-dimensional forms via ChemBioOffice 2008 (CambridgeSoft Inc., Cambridge, MA, USA). Energy minimization of TCM compounds was performed using MM2 forcefield in ChemBioOffice.

The crystal structure of M2 proton channel was downloaded from Protein Data Bank (PDB code: 3C9J (53)). Amantadine presented in the protein crystal was taken out, but was re-docked back into M2 protein in subsequent steps. All water molecules and other non-biopolymer heteroatoms were removed.

### Docking Screening

Docking was conducted in Discovery Studio v2.5 0.9164 (Accelrys Inc, San Diego, USA). Forcefield of Chemistry at Harvard Macromolecular Mechanics (CHARMm) was applied to both M2 protein and small molecules prior to docking process. LigandFit program of Discovery Studio was used for docking while scoring functions, Dock Score, LigScore1 (54), LigScore2 (54), PLP1 (55), PLP2 (56) and PMF (57), were employed for evaluating molecule binding affinity. Amantadine binding location was defined as binding site, and TCM compounds and amantadine were docked into it. The scoring function outputs for amantadine were used as control for filtering TCM compounds.

### De Novo Evolution and Lipinski's Rule of Five

TCM compounds with higher docking scores than amantadine were selected from the previous step. Their scaffolds were then modified and developed into derivatives in *de novo* evolution process. In *de novo* evolution, Ludi algorithm was employed to generate possible interaction sites within the ligand binding location. Fragments that can complement the receptor while also form favorable interaction with the Ludi interaction sites are fused or linked to the docked TCM ingredients. The generated derivatives were docked back into the M2 protein to examine their binding affinities. Lipinski's Rule of Five was used to filter out compounds that may not be orally active.

### Molecular Dynamics Simulation

The top docked TCM derivatives were selected for molecular dynamics simulations. The simulations were initiated from M2-derivative complex coordinates. All simulations were carried out with Discovery Studio v2.5. The CHARMm forcefield was applied to both protein and small molecules. The protein-ligand systems were solvated in a cubic box of water molecules (a total of 6056 water molecules) with explicit periodical boundary condition. All the protein and TCM atoms are at a distance equal or greater than 7 Å from the boundary. The particle-mesh Ewald (PME) method was used for electrostatics calculations (58). The time step was 1 fs, and the SHAKE algorithm was used to constrain bonds containing hydrogen. The frequency of velocity adjustment for each particle was set to every 50 steps.

Initially, the M2-derivative system underwent 500 steps of steepest descent minimization and 500 steps of conjugate gradient minimization. The energy minimization step was followed by heating, equilibration and production. The whole system

**Table I**  
The top 6 candidates docking results of M2 Protein.

Name	DS*	LigS1	LigS2	-PLP1	-PLP2	-PMF
Quinic acid	42.95	4.54	4.49	49.70	58.33	30.00
Genipin	42.18	3.69	4.81	47.67	47.84	44.14
Syringic acid	41.60	2.25	3.61	49.35	49.94	97.62
Cucurbitine	39.94	4.11	4.11	47.50	50.29	46.30
Fagarine	39.39	1.35	4.16	79.35	71.18	98.43
Methyl isoferulate	38.68	2.69	4.41	52.43	46.99	47.83
Amantadine	33.87	0.89	3.70	28.50	26.60	-2.90

The control, amantadine, is in gray shade.

\*Dock Score.

was heated from initial temperature of 50K to 310 K in 20 ps. The equilibration was run in 310K for 100 ps without restrained. During production, the simulation was performed in NVT ensemble at 310 K with temperature coupling decay time of 5 ps. The production was run until the root mean square deviation (RMSD) of the whole protein-ligand complex reached a plateau. The snapshots from the production period were saved every 2.5 ps.

To evaluate protein and ligand conformation changes, RMSD was computed for the entire protein molecule using the starting structure as reference. Hydrogen bonding between the M2 protein and the TCM derivative was monitored and analyzed over the course of the simulation. The cutoff for hydrogen bonding interaction was set to 2.5 Å. Percentage of hydrogen bond occupancy was calculated as the number of hydrogen bond appearances over the number of conformations sampled during the molecular dynamics simulation.

## Results and Discussion

### Docking Screening

Docking and scoring of TCM compounds and amantadine enable us to evaluate docking conformations and binding affinity of these small molecules in M2. Of all the proposed adamantane inhibitor binding sites and inhibitor mechanisms, the direct pore blocking strategy of amantadine, as supported by the crystal structure

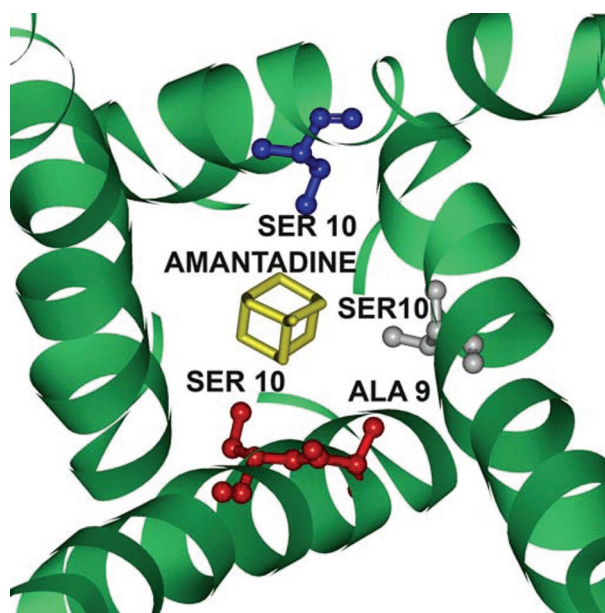


**Figure 2:** The docking pose of amantadine (control) in M2 protein.

**Table II**  
The top 10 derivatives from *de novo* evolution.

**Potent Inhibitor Design  
Against H1N1 Swine  
influenza**

Name	DS	LigS1	LigS2	-PLP1	-PLP2	-PMF
Methyl isoferulate_1	57.17	5.01	5.86	71.84	73.26	92.77
Genipin_1	55.61	5.40	6.01	81.22	84.53	64.67
Genipin_2	54.84	5.22	5.87	77.03	83.09	67.74
Methyl isoferulate_2	54.64	4.34	5.86	67.10	63.13	97.83
Genipin_6	53.60	4.64	5.66	70.32	72.96	70.09
Genipin_3	53.00	5.34	5.89	79.49	82.95	63.48
Limettin_9	52.49	2.91	5.36	63.19	57.44	93.61
Limettin_7	52.24	1.96	4.90	67.05	59.18	83.53
Genipin_4	52.21	4.99	5.60	68.01	68.15	61.37
Genipin_8	51.72	4.10	5.37	61.48	61.81	58.06
Amantadine	33.87	0.89	3.70	28.50	26.60	-2.90

The control, amantadine, is in gray shade.

\*Dock Score.

used in this study, is the most well studied and recognized. Therefore, we chose the amantadine binding site as the TCM docking site. The outputs of scoring functions are shown in Table I. Only the top six TCM compounds, as ranked by Dock Score, are shown. Based on our past experiences, Dock Score has the highest positive correlation with compound bioactivity (32), and therefore, we used Dock Score for ranking purpose. LigScore1, LigScore2, PLP1, PLP2 and PMF are shown in Table I as additional references.

The control, amantadine, is a well example of the predictivity of scoring functions. The crystal structure used in our study (Figure 2), as well as NMR structure solved by Schnell and Chou (59), both confirmed that the M2 channel inner lining is highly hydrophilic and is energetically unfavorable for the hydrophobic, adamantane-based amantadine. As reflected in scoring results, amantadine has relative low Dock Score, LigScore (which accounts for polar attraction), -PLP (which evaluates hydrogen bond interaction) and -PMF (which compute Helmholtz free interaction energies). In contrast, the top TCM compounds resulted from docking all contain hydrophilic groups that are more favorable for interacting M2 proton channel residues and, therefore, should have stronger hydrogen bond interaction. Judging by their scoring function outputs, these TCM compounds are hypothesized to have higher binding affinity for M2 protein.

#### *De Novo Evolution and Lipinski's Rule of Five*

From docking screening, a total of 34 compounds with Dock Score higher than amantadine were selected for *de novo* evolution, which generated 93 derivatives. These passed the Lipinski's rule of five screening were re-docked back to M2 proton pore to evaluate docking conformations and scoring function outputs (shown in Table II).

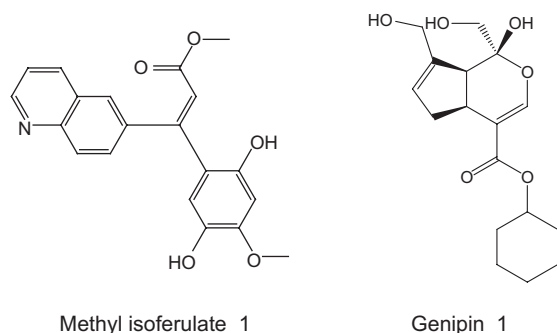


**Figure 3:** The structure of top 2 compounds from *de novo* Evolution.

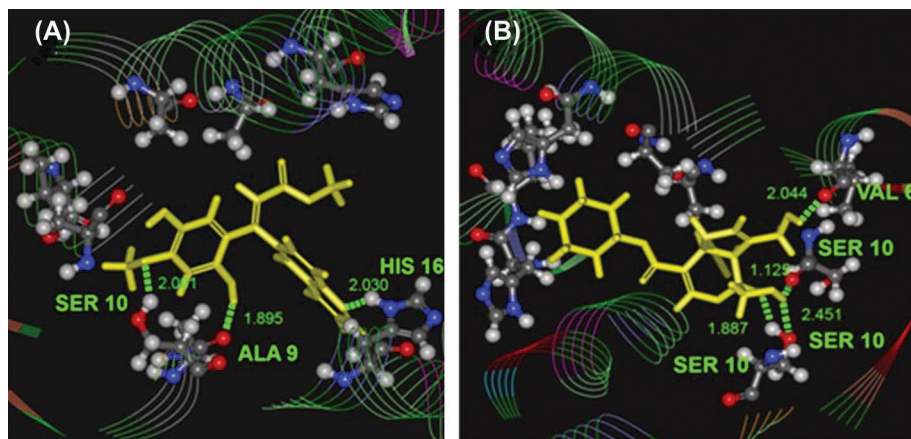


**Figure 4:** The docking pose of (A) methyl isoferulate\_1, and (B) genipin\_1.

The top 10 derivatives, which all have scoring results better than the control, consist of compounds from methyl isoferulate (constituents of *Phellodendron amurense* var. *wilsonii* (60)), genipin (constituents of *Gardenia jasminoides* fruit (61)) and limettin (constituents of Citrus (62)). Of the three, genipin is most well known as cross-linker in protein-linking (63). Past studies have also reported the anti-hepatitis B virus activity of genipin derivative (64). However, all three compounds have not been studied before for anti-influenza activity. To our best knowledge, this is the first study to investigate the anti-influenza potential of these three compounds.

Two-dimensional structures of the top two TCM derivatives are shown in Figure 3, and their docking conformations are shown in Figure 4. These TCM derivatives differ from amantadine in containing more hydrogen bond donors and acceptors that could form interactions with hydrophilic residues of the M2 channel. However, similar to amantadine, all TCM derivatives still have hydrophobic substructures, such as cyclohexane, in addition to hydrophilic groups. For methyl isoferulate\_1-M2 complex, hydrogen bond interactions can be seen between the ligand and protein residues, Ser10 and Ala9 (Figure 4(a)). A third hydrogen bond interaction

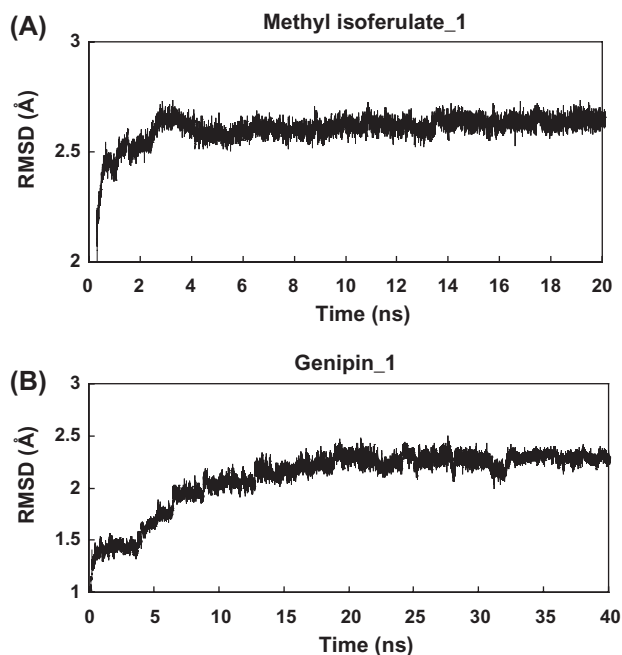


**Figure 5:** Root-mean-square deviation of M2-ligand complexes (A) methyl isoferulate\_1 from 20 ns MD simulation and (B) genipin\_1 from 40 ns MD simulation.



**Table III**  
Summary of hydrogen bonds statistics after molecular dynamics simulation.

	Max. Distance	Min. Distance	Ave. Distance	% of Occupancy
A:SER10 HG-Methyl isoferulate_1 O24	3.846	1.668	2.282	73.09%
D:HIS16 HD1-Methyl isoferulate_1 O7	3.715	1.624	1.942	98.54%
A:SER10 OG-Methyl isoferulate_1 H25	2.990	1.659	2.018	99.98%
C:ALA9 O-Methyl isoferulate_1 H43	3.661	1.697	2.402	72.06%
A: ALA9 O-Genipin_1 H12	3.485	1.832	2.494	55.64%
A: SER10 HG-Genipin_1 O26	3.814	1.672	2.211	92.89%

## Potent Inhibitor Design Against H1N1 Swine influenza

is established between the quinoline group of ligand and His16 side chain (Figure 4(A)). For genipin\_1-M2 complex, hydrogen bond interactions are mostly found between ligand and Ser10 (Figure 4(B)).

### Molecular Dynamics Simulation

To further analyze protein-ligand interaction, we selected the top two *de novo* compounds for molecular dynamics simulation. The overall goal of this simulation step was to account for protein flexibility and movement that cannot be achieved in the docking simulation. For methyl isoferulate\_1-M2 complex, the production step was run for 20 ns, and a plateau in whole molecule RMSD (2.6 Å) was reached after 4 ns of simulation (Figure 5(A)). Interestingly, the

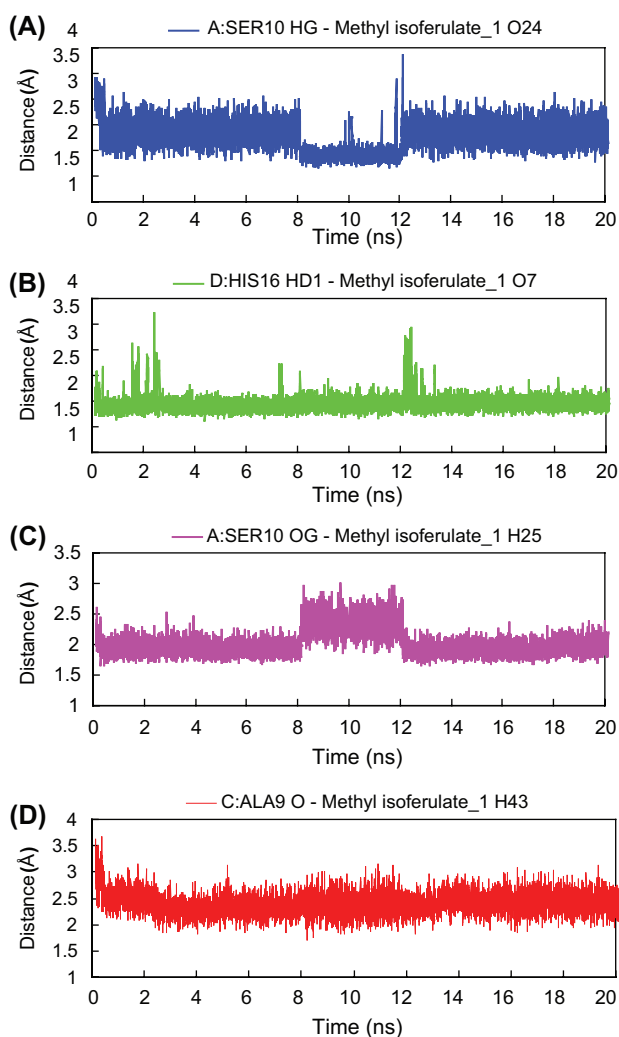


**Figure 6:** Hydrogen bond distance of M2-methyl isoferulate\_1 complex during 20 ns MD simulation.

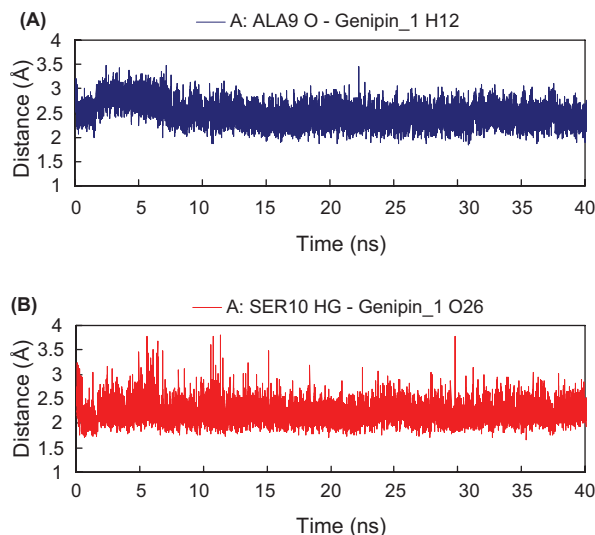


**Figure 7:** Hydrogen bond distance of M2-genipin\_1 complex during 40 ns MD simulation.

genipin\_1-M2 complex took a longer simulation time out of entire 40 ns production run to reach dynamics equilibrium (Figure 5(B)), but the complex stabilized at 2.3 Å, which deviated less than methyl isoferulate\_1 complex from the starting crystal structure. These results suggest that the methyl isoferulate\_1 complex undergoes a rather rapid conformational change compared to genipin\_1 complex. We, therefore, hypothesize that methyl isoferulate\_1 can more efficiently induce M2 conformational changes, such as by interacting with key residue His16 to close the M2 channel.

We have analyzed the hydrogen-bond interactions and calculated the length of hydrogen bond for the two TCM derivative-M2 complexes. For methyl isoferulate\_1 complex, four hydrogen bonds are observed, with percent of occupancy over 50 of the entire simulation (Table III). The interaction between the protonated nitrogen of His16 imidazole ring (chain D) and the carbonyl group of methyl isoferulate\_1 is one of the most stable hydrogen bond interactions throughout the simulation with distance averaging 1.942 Å (Figure 6(B)). The interaction between hydroxyl group of methyl isoferulate\_1 and of Ser10 side chain, however, is more interesting with noticeable changes during the period of 8-12ns, hinting a possible fluctuation in M2 chain A conformation at that time (Figure 6(A) and (C)). As for hydrogen bonding between carbonyl backbone of Ala9 (chain C) and methyl isoferulate\_1, the distance appears to be largely fluctuating around 2.5 Å, suggesting substantial changes in M2 chain C. For genipin\_1-M2 complex, two hydrogen bonds are observed (Table III). Their hydrogen bond distances are shown in Figure 7(A) and (B). The interacting protein residues (Ala9 and Ser10) are similar to those observed in methyl isoferulate\_1 complex but with large fluctuation from the averaging distances. Based on the results from genipin\_1 and methyl isoferulate-M2 complex, it appears that interactions to Ala9 and Ser10 of M2 protein are important for inhibitory activity of the TCM derivatives.

Snapshots from molecular dynamics simulations are shown in Figures 8 and 9 for methyl isoferulate\_1 and genipin\_1, respectively. A comparison between the poses obtained from docking and from molecular dynamics simulation shows that substantial changes in binding conformations have occurred. Initial docking conformation of methyl isoferulate\_1 has a hydrogen bond interaction between the nitrogen of quinoline ring and protonated imidazole ring of His16. This interaction, however, is later shifted to between the more electronegative carbonyl group of methyl isoferulate\_1 and His16 (Figure 8(A)) and is later maintained to the end of simulation run (Figure 8(B)). For genipin\_1, several hydrogen bond



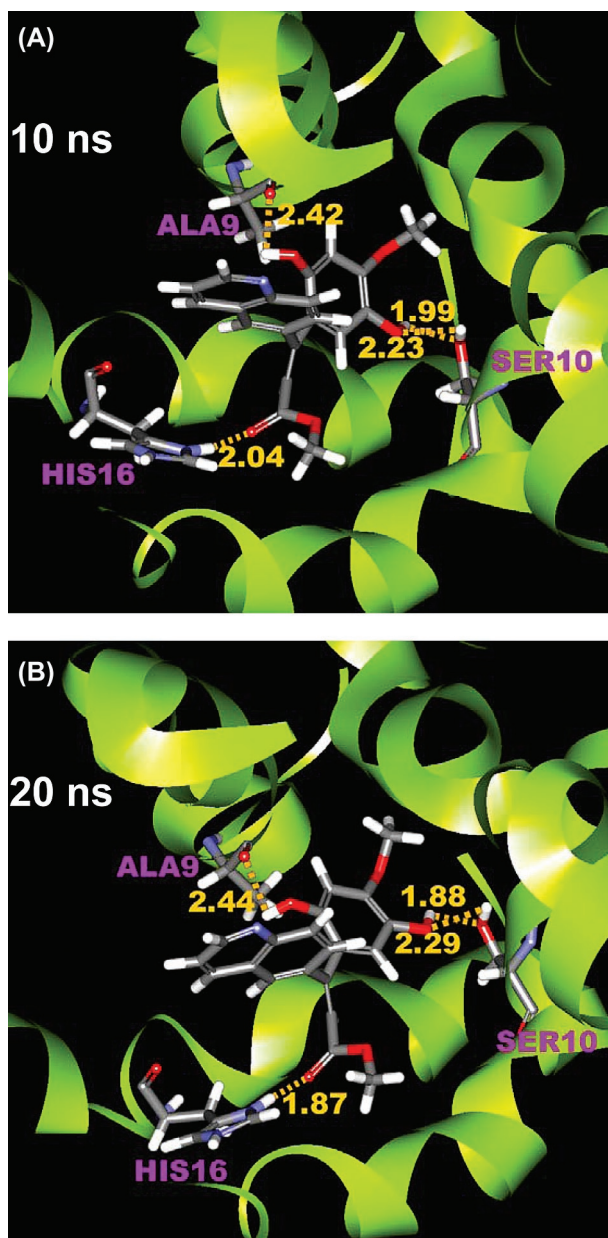


**Figure 8:** Conformation of methyl isoferulate\_1-M2 complex at (A) 10 ns and (B) 20 ns. Protein residues, Ala9 (chain C), Ser10 (chain A) and His16 (chain D), are labeled in purple. The length of hydrogen bonds is shown in yellow.

interactions of the ligand to Ser10 residues can be found after docking, but most interactions diminish after the simulation (Figure 9(A-B)). The hydrogen bond interaction of genipin\_1 to Ala9 may be temporarily interrupted at 20 ns (Figure 9(A)), but, as shown in Figure 7(A), this interaction is constantly fluctuating. These results suggest that the initial receptor-ligand interaction observed after docking can be limited due to the receptor rigid docking algorithm and that the conformations and interactions observed after simulation runs are more energetically favored and should be better representation of derivative binding conformation in the receptor.

### **Conclusion**

We have performed docking and molecular dynamics simulation studies to search for TCM constituents that have potential M2 channel inhibitory activity. Our docking simulation gives six TCM compounds that have better predicted binding affinity

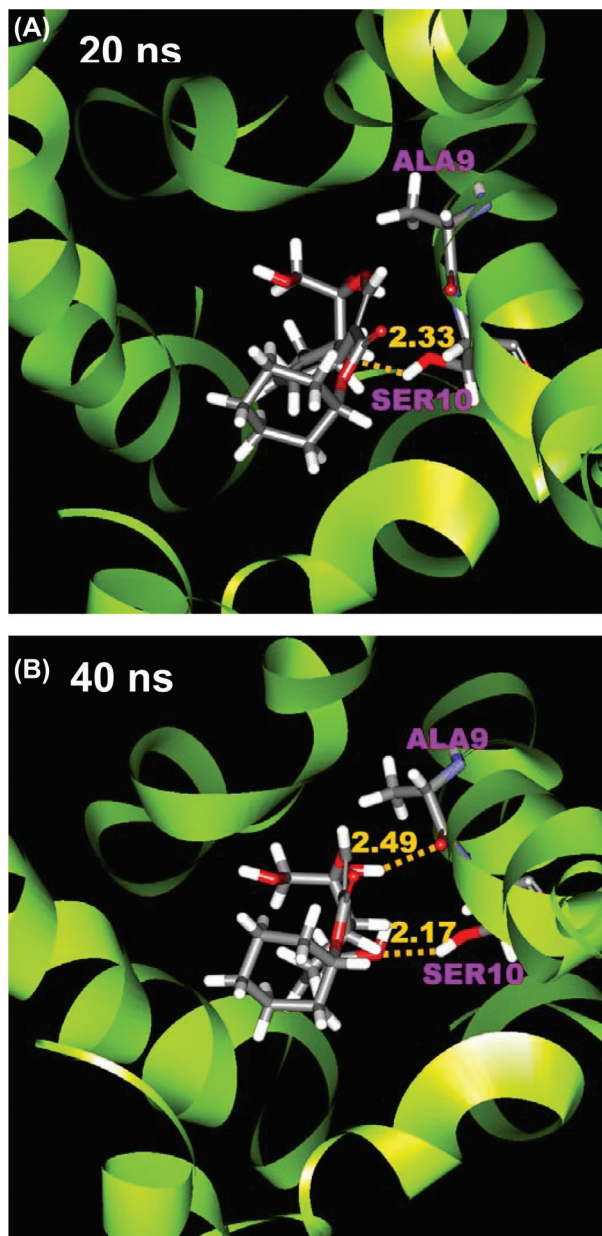


**Figure 9:** Conformation of genipin\_1-M2 complex at (A) 20 ns and (B) 40 ns. Protein residues, Ala9 (chain A) and Ser10 (chain A), are labeled in purple. The length of hydrogen bond is shown in yellow.

than the control, amantadine. Further, *de novo* simulation and docking of derivatives suggest that genipin, methyl isoferulate, and their derivatives as possible M2 inhibitors. Methyl isoferulate\_1 and genipin\_1 form hydrogen bond interactions with M2 residues, Ala9 and Ser10, during their respective 20 ns and 40 ns molecular simulation runs, suggesting that ligand interaction to these two residues could be critical for inhibitor activity.

#### **Acknowledgements**

The research was supported by grants from the National Science Council of Taiwan (NSC 99-2221-E-039-013-), China Medical University (CMU98-TCM, CMU99-S-02) and Asia University (CMU98-ASIA-09). This study is also supported in part by Taiwan Department of Health Clinical Trial and Research Center of Excellence (DOH99-TD-B-111-004) and Taiwan Department of Health Cancer Research Center of Excellence (DOH99-TD-C-111-005). We are grateful to the National Center of High-performance Computing for computer time and facilities.

1. A. C. Hurt, J. Ernest, Y. M. Deng, P. Iannello, T. G. Besselaar, C. Birch, P. Buchy, M. Chittaganpitch, S. C. Chiu, D. Dwyer, A. Guigon, B. Harrower, I. P. Kei, T. Kok, C. Lin, K. McPhie, A. Mohd, R. Olveda, T. Panayotou, W. Rawlinson, L. Scott, D. Smith, H. D'Souza, N. Komadina, R. Shaw, A. Kelso, and I. G. Barr. *Antiviral Res* 83, 90-93 (2009).
2. S. D. Cady, W. B. Luo, F. H. Hu, and M. Hong. *Biochemistry* 48, 7356-7364 (2009).
3. G. Y. Chuang, D. Kozakov, R. Brenke, D. Beglov, F. Guarnieri, and S. Vajda. *Biophys J* 97, 2846-2853 (2009).
4. M. Yi, T. A. Cross, and H. X. Zhou. *J Phys Chem B* 112, 7977-7979 (2008).
5. N. A. Ilyushina, E. A. Govorkova, and R. G. Webster. *Virology* 341, 102-106 (2005).
6. F. G. Hayden. *N Engl J Med* 354, 785-788 (2006).
7. E. D. Akten, S. Cansu, and P. Doruker. *J Biomol Struct Dyn* 27, 13-25 (2009).
8. A. M. Andrianov. *J Biomol Struct Dyn* 26, 445-454 (2009).
9. A. M. Andrianov, and I. V. Anishchenko. *J Biomol Struct Dyn* 27, 179-193 (2009).
10. G. Ompraba, D. Velmurugan, P. A. Louis, and Z. A. Rafi. *J Biomol Struct Dyn* 27, 489-499 (2010).
11. M. T. Cambria, D. Di Marino, M. Falconi, S. Garavaglia, and A. Cambria. *J Biomol Struct Dyn* 27, 501-509 (2010).
12. E. F. F. da Cunha, E. F. Barbosa, A. A. Oliveira, and T. C. Ramalho. *J Biomol Struct Dyn* 27, 619-625 (2010).
13. C. Meynier, F. Guerlesquin, and P. Roche. *J Biomol Struct Dyn* 27, 49-57 (2009).
14. S. Mohan, J. J. P. Perry, N. Poulouse, B. G. Nair, and G. Anilkumar. *J Biomol Struct Dyn* 26, 455-464 (2009).
15. T. C. Ramalho, M. S. Caetano, E. F. F. da Cunha, T. C. S. Souza, and M. V. J. Rocha. *J Biomol Struct Dyn* 27, 195-207 (2009).
16. J. Sille, and M. Remko. *J Biomol Struct Dyn* 26, 431-444 (2009).
17. H. R. Bairagya, B. P. Mukhopadhyay, and K. Sekar. *J Biomol Struct Dyn* 27, 149-158 (2009).
18. B. Jin, H. M. Lee, and S. K. Kim. *J Biomol Struct Dyn* 27, 457-464 (2010).
19. C. Koshiy, M. Parthiban, and R. Sowdhamini. *J Biomol Struct Dyn* 28, 71-83 (2010).
20. F. Mehrnejad and M. Zarei. *J Biomol Struct Dyn* 27, 551-559 (2010).
21. S. Roy and A. R. Thakur. *J Biomol Struct Dyn* 27, 443-455 (2010).
22. A. Sharadadevi and R. Nagaraj. *J Biomol Struct Dyn* 27, 541-550 (2010).
23. S. Sharma, U. B. Sonavane, and R. R. Joshi. *J Biomol Struct Dyn* 27, 663-676 (2010).
24. Y. Tao, Z. H. Rao, and S. Q. Liu. *J Biomol Struct Dyn* 28, 143-157 (2010).
25. M. J. Aman, H. Karauzum, M. G. Bowden, and T. L. Nguyen. *J Biomol Struct Dyn* 28, 1-12 (2010).
26. J. F. Varughese, J. M. Chalovich, and Y. Li. *J Biomol Struct Dyn* 28, 159-173 (2010).
27. J. P. Zhang. *J Biomol Struct Dyn* 27, 159-162 (2009).
28. L. H. Zhong, and J. M. Xie. *J Biomol Struct Dyn* 26, 525-533 (2009).
29. A. Cordomi, and J. J. Perez. *J Biomol Struct Dyn* 27, 127-147 (2009).
30. Y. Yuan, M. H. Knaggs, L. B. Poole, J. S. Fetrow, and F. R. Salsbury, Jr. *J Biomol Struct Dyn* 28, 51-70 (2010).
31. J. Wiesner, Z. Kriz, K. Kuca, D. Jun, and J. Koca. *J Biomol Struct Dyn* 28, 393-403 (2010).
32. C. Y. C. Chen. *J Biomol Struct Dyn* 27, 271-282 (2009).
33. H. J. Huang, K. J. Lee, H. W. Yu, H. Y. Chen, F. J. Tsai, and C. Y. Chen. *J Biomol Struct Dyn* 28, 187-200 (2010).
34. H. J. Huang, K. J. Lee, H. W. Yu, C. Y. Chen, C. H. Hsu, H. Y. Chen, F. J. Tsai, and C. Y. C. Chen. *J Biomol Struct Dyn* 28, 23-37 (2010).
35. C. Y. Chen, and C. Y. C. Chen. *J Mol Graph Model* 29, 21-31 (2010).
36. H. J. Huang, C. Y. Chen, H. Y. Chen, F. J. Tsai, and C. Y. C. Chen. *J Taiwan Inst Chem Eng* 41, 352-359 (2010).
37. C. Y. C. Chen. *J Biomol Struct Dyn* 27, 627-640 (2010).
38. C. Y. C. Chen. *J Taiwan Inst Chem Eng* 41, 143-149 (2010).
39. C. Y. Chen, H. J. Huang, F. J. Tsai, and C. Y. C. Chen. *J Taiwan Inst Chem Eng* 41, 8-15 (2010).
40. C. Y. C. Chen. *J Mol Graphics Model* 28, 261-269 (2009).
41. C. Y. Chen, Y. H. Chang, D. T. Bau, H. J. Huang, F. J. Tsai, C. H. Tsai, and C. Y. C. Chen. *J Biomol Struct Dyn* 27, 171-178 (2009).
42. C. Y. Chen, Y. H. Chang, D. T. Bau, H. J. Huang, F. J. Tsai, C. H. Tsai, and C. Y. C. Chen. *Acta Pharmacol Sin* 30, 1186-1194 (2009).
43. C. Y. C. Chen. *J Taiwan Inst Chem Eng* 40, 155-161 (2009).
44. C. Y. C. Chen. *J Taiwan Inst Chem Eng* 40, 55-69 (2009).
45. C. Y. C. Chen. *J Taiwan Inst Chem Eng* 40, 36-47 (2009).
46. C. Y. C. Chen. *J Chin Inst Chem Eng*, 39, 663-671 (2008).
47. C. Y. C. Chen. *J Chin Inst Chem Eng*, 39, 617-624 (2008).
48. C. Y. C. Chen, Y. F. Chen, C. H. Wu, and H. Y. Tsai. *J Biomol Struct Dyn* 26, 57-64 (2008).

49. C. Y. C. Chen. *J Chin Inst Chem Eng* 39, 291-299 (2008).
50. C. Y. C. Chen, G. W. Chen, and W. Y. C. Chen. *J Chin Chem Soc* 55, 297-302 (2008).
51. Y. C. Chen and K. T. Chen. *Acta Pharmacol Sin* 28, 2027-2032 (2007).
52. Y. C. Chen. *J Chin Chem Soc* 54, 653-658 (2007).
53. A. L. Stouffer, R. Acharya, D. Salom, A. S. Levine, L. Di Costanzo, C. S. Soto, V. Tereshko, V. Nanda, S. Stayrook, and W. F. DeGrado. *Nature* 451, 596-599 (2008).
54. A. Krammer, P. D. Kirchhoff, X. Jiang, C. M. Venkatachalam, and M. Waldman. *J Mol Graph Model* 23, 395-407 (2005).
55. D. K. Gehlhaar, G. M. Verkhivker, P. A. Rejto, C. J. Sherman, D. B. Fogel, L. J. Fogel, and S. T. Freer. *Chem Biol* 2, 317-324 (1995).
56. A. L. Parrill, M. Rami Reddy, American Chemical Society. Division of Computers in Chemistry., and American Chemical Society. Meeting. *Rational drug design: novel methodology and practical applications*. (American Chemical Society, 1999).
57. I. Muegge and Y. C. Martin. *J Med Chem* 42, 791-804 (1999).
58. T. Darden and D. L. York. *J Chem Phys* 98, 10089-10092 (1981).
59. J. R. Schnell and J. J. Chou. *Nature* 451, 591-595 (2008).
60. Q. Ding, L. Huo, J. Y. Yang, W. Xia, Y. Wei, Y. Liao, C. J. Chang, Y. Yang, C. C. Lai, D. F. Lee, C. J. Yen, Y. J. Chen, J. M. Hsu, H. P. Kuo, C. Y. Lin, F. J. Tsai, L. Y. Li, C. H. Tsai, and M. C. Hung. *Cancer Res* 68, 6109-6117 (2008).
61. T. N. Chang, G. J. Huang, Y. L. Ho, S. S. Huang, H. Y. Chang, and Y. S. Chang. *Am J Chin Med* 37, 797-814 (2009).
62. E. Gorgus, C. Lohr, N. Raquet, S. Guth, and D. Schrenk. *Food Chem Toxicol* 48, 93-98 (2010).
63. Y. H. Chang, J. S. Yang, J. L. Yang, C. L. Wu, S. J. Chang, K. W. Lu, J. J. Lin, T. C. Hsia, Y. T. Lin, C. C. Ho, W. G. Wood, and J. G. Chung. *Biosci Biotechnol Biochem* 73, 2589-2594 (2009).
64. M. Schuchmann and P. R. Galle. *Eur J Gastroenterol Hepatol* 13, 785-790 (2001).

Date Received: August 12, 2010

Communicated by the Editor Ramaswamy H. Sarma